Barkas Effect for Antiproton Stopping in H_2

E. Lodi Rizzini,[1,*] A. Bianconi,[1] M. P. Bussa,[1] M. Corradini,[1] A. Donzella,[1] L. Venturelli,[1] M. Bargiotti,[2] A. Bertin,[2] M. Bruschi,[2] M. Capponi,[2] S. De Castro,[2] L. Fabbri,[2] P. Faccioli,[2] D. Galli,[2] B. Giacobbe,[2] U. Marconi,[2] I. Massa,[2] M. Piccinini,[2] M. Poli,[2] N. Semprini Cesari,[2] R. Spighi,[2] V. Vagnoni,[2] S. Vecchi,[2] M. Villa,[2] A. Vitale,[2] A. Zoccoli,[2] O. E. Gorchakov,[3] G. B. Pontecorvo,[3] A. M. Rozhdestvensky,[3] V. I. Tretyak,[3] C. Guaraldo,[4] C. Petrascu,[4] F. Balestra,[5] L. Busso,[5] O. Y. Denisov,[5] L. Ferrero,[5] R. Garfagnini,[5] A. Grasso,[5] A. Maggiora,[5] G. Piragino,[5] F. Tosello,[5] G. Zosi,[5] G. Margagliotti,[6] L. Santi,[6] and S. Tessaro[6]

[1]*Dipartimento di Chimica e Fisica per l'Ingegneria e per i Materiali, Università di Brescia, Brescia and INFN, gruppo di Brescia, Brescia, Italy*

[2]*Dipartimento di Fisica, Università di Bologna and INFN, Sezione di Bologna, Bologna, Italy*

[3]*Joint Institute for Nuclear Research, Dubna, Moscow, Russia*

[4]*Laboratori Nazionali di Frascati dell'INFN, Frascati, Italy*

[5]*Dipartimento di Fisica Generale "A. Avogadro," Università di Torino and INFN, Sezione di Torino, Torino, Italy*

[6]*Istituto di Fisica, Università di Trieste and INFN, Sezione di Trieste, Trieste, Italy*

(Received 15 April 2002; published 10 October 2002)

We report the stopping power of molecular hydrogen for antiprotons of kinetic energy above the maximum ($\approx$ 100 keV) with the purpose of comparing with the proton one. Our result is consistent with a positive difference in antiproton-proton stopping powers above $\approx$ 250 keV and with a maximum difference between the stopping powers of 21% $\pm$ 3% at around 600 keV.

DOI: 10.1103/PhysRevLett.89.183201 PACS numbers: 34.50.Bw

A subject that in the last two decades has raised much interest in the field of charged-particle interaction with matter is the antiproton stopping power. With the advent of the Low Energy Antiproton Ring (LEAR) at CERN, the Obelix Collaboration has for the first time measured at low energies the $\bar{p}$ energy loss per unit path length (the stopping power) in gaseous H_2, D_2, and He, i.e., the simplest molecules and atom [1–3]. For H_2 and D_2 the behavior of the stopping power was determined for $\bar{p}$ kinetic energies ranging from about 1.1 MeV down to the capture energy. The evidence of strong differences in the nuclear stopping power was inferred in [3], and it is in agreement with the Wightman prediction [4]. In the electronic domain a negative difference between the $\bar{p}$ and p behaviors near the maximum (at about 100 keV), known as Barkas effect [5], was clearly observed and evaluated. Moreover, at energies higher than 200–300 keV, the $\bar{p}$ stopping power seems to exceed that of the proton [1,2].

This phenomenon is related to theories [6] on the cross sections for energy loss in the case of excitation and ionization produced by positive or negative bare ions. Negative projectiles are predicted to have cross sections higher than those determined by the first Born approximation. Quinteros and Reading [6] dealt with a number of arguments relevant to atomic collisions and the processes involved (mainly binding energy and polarization of the system formed by at least two atomic electrons), and they nicely termed the phenomenon at issue the "bus stop effect." The calculations of Ermolaev [7,8] have apparently also confirmed this effect. However, the experimental evidence hitherto collected is rather weak (see [9] for the measurements of the cross section for single ionization of molecular hydrogen by positron and electron impact).

To improve and quantify our knowledge on the Barkas effect in molecular hydrogen [10] we use the data collected by the Obelix detector. Our starting point is the behavior of the $\bar{p}$ electronic stopping power function [1,2], supplemented with the information on the nuclear stopping power [3] and with a new hypothesis on the capture energy [11]. Differently from other experiments based on the direct differential method, we derive the stopping power by an integral method which combines the projectile-range distributions with the distributions of slowing down times. This method features high sensitivity to the energy losses of very slow projectiles.

The Obelix apparatus is composed of a cylindrical gas target 75 cm long surrounded by a scintillator barrel and jet drift chambers to measure the time and the spatial coordinates of the vertex of the annihilation event inside the target with an accuracy of 1 ns and 1 cm, respectively. Details about the apparatus and the measurement technique may be found in [1–3].

The $\bar{p}$ monochromatic beam produced by the LEAR facility in the slow extraction mode (with about a single $\bar{p}$ every microsecond) is suitably degraded in order to have a beam energy continuously distributed from $E_i^{\min} \simeq 0$ up to $E_i^{\max} \simeq 1.1$ MeV at the entrance of the target. Therefore $\bar{p}$ annihilations at rest are spread along the whole gaseous target at all the densities used.

To evaluate the $\bar{p}$ stopping power $[S(E)]$ in H_2, we searched for the best fit of the experimental annihilation points with a function $t = f(z)$ obtained by the simultaneous solution of both space $[R(E)]$ and time $[t(E)]$

integral relationships:

$$R(E_i) = \int_{E_{\text{cap}}}^{E_i} \frac{dE}{S(E)}, \tag{1}$$

$$t(E_i) = \int_{E_{\text{cap}}}^{E_i} \frac{dE}{\upsilon S(E)} = \langle t_a \rangle - \langle t_{\text{cas}} \rangle, \tag{2}$$

E_i being the $\bar{p}$ initial laboratory kinetic energy, υ the instantaneous velocity, and $\langle t_a \rangle$ the $\bar{p}$ mean annihilation time, all variable along the target. The $\bar{p}$ capture energy by the target atom E_{cap} and the mean cascade time $\langle t_{\text{cas}} \rangle$, on the contrary, are constant for each pressure along the target.

Starting from the results of the study by Andersen and Ziegler on the proton stopping power [12], we used for the evaluation of the $\bar{p}$ electronic stopping power the simple interpolation formula $S(E)$ given by $1/S = 1/S_l + 1/S_h$, where S_l (low energy stopping) is $S_l = \alpha E^{\beta}$ and S_h (high energy stopping) is $S_h = (242.6/E)\ln(1 + \gamma/E + 0.1159E)$. The S_h and E units are eV 10^{-15} atoms^{-1} cm^2 and keV, respectively [13]. The values obtained were $\alpha = 1.25$, $\beta = 0.3$, $\gamma = 4 \times 10^5$, respectively. The fitting formula obtained with these three parameters asymptotically agrees with the nuclear stopping power at very low energies, and with the Bethe formula at high energies, which is derived in the first Born approximation.

For the present analysis we use the data samples collected with a H_2 target at the pressures 150, 10, 9.8, 5.8, 5, 3.4, and 2 mbar at room temperature. The uncertainty in the pressure values amounts to a few percent.

By decreasing the target density we increase the sensitivity along the target of the $\bar{p}$ stopping power measurement. In Fig. 1 we show all the data together with the best fit stopping power function described above. We display our different curves $t = f(z)$ for all the pressure samples in a single plot, setting to zero the cascade time and multiplying both z and t by the pressure.

If one wishes to negate the inversion of the Barkas effect one may try to find a $S(E)$ behavior like that of the proton beyond the $\bar{p}$ maximum, and the corresponding $t = f(z)$ function must fit the experimental data. Therefore, in the present analysis we compare our best stopping power function (curve 1) with other possible $S(E)$ behaviors to evaluate the possible effect (curves 2, 3, 4); see Fig. 2(a). A physically significant behavior of the $\bar{p}$ stopping power without intersection with the proton stopping power above the maximum necessarily requires behaviors like that of curves 2 and 3 in Fig. 2(a), with maxima shifted to the left. Except for γ, the coefficients of S_h in the interpolation formula for $S(E)$ depend on the general properties of the target materials.

In Fig. 3 we show for some pressures the z versus t behavior relative to these different $S = S(E)$ functions, including the best fit function of Fig. 1 (curve 1), with the experimental points superimposed. The plots refer to a capture energy $E_{\text{cap}} = 40$ eV. We also present in Fig. 3 the $\bar{p}$ annihilation points for different $\bar{p}$ initial kinetic energies. The change in sensitivity of our technique to the

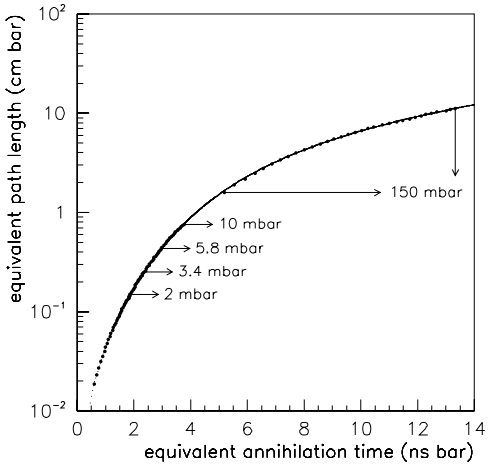

FIG. 1. Equivalent $\bar{p}$ path length versus equivalent mean annihilation time with the best fit curve described in the text, for various pressures with $E_{\text{cap}} = 40$ eV. For each pressure the arrow indicates the position of the last annihilation vertex in the target. For 150 mbar pressure the arrows indicate the interval between the first and last experimental annihilation vertices.

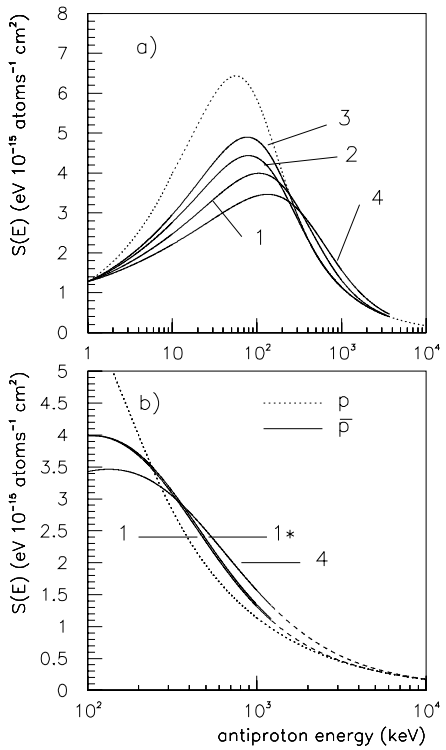

FIG. 2. (a) $\bar{p}$ best stopping power function in H_2 (curve 1) with the other analyzed $\bar{p}$ stopping power functions (curves 2–4); the proton behavior superimposed (dotted). (b) Enlargement of (a) in the region above the maximum. Curves 1, 1*, and 4: see text.

different $\bar{p}$ initial energies with the target pressures is evident. Curves 2 and 3 (Figs. 3(b) and 3(c), respectively) appear not to agree with the experimental data. In fact, the experimental slopes are lower than the phenomenological ones at the pressures 3.4 and 10 mbar and are higher for the 150 mbar data. Such a difference increases from curve 2 to curve 3. Considering the plot for 10 mbar in Fig. 3(c), where the differences are better observable, we conclude that we need a decrease of the proposed $S(E)$ function (curve 3) to optimize the annihilation time for $\bar{p}$s with initial kinetic energies around and below the maximum. Moreover, we also check other behaviors, as that of curve 4 in Fig. 2(a), which for higher initial $\bar{p}$ kinetic energies show an even higher $\bar{p}$ stopping as compared to curve 1. The results are shown in Fig. 3(d). The slopes for the experimental points are now higher than the phenomenological ones at 3.4 and 10 mbar.

What we present here in Figs. 3 has been carefully evaluated with a χ^2 statistical analysis and confirms the previous estimates for α, β, and γ.

To quantify the Barkas effect we investigate the parameters of the $S(E)$ function by checking different $S(E)$ behaviors very similar to that of curve 1, such as that of curve 1* in Fig. 2(b). Thus, in Fig. 2(b) we show for the energy region above the maximum stopping power the proton behavior and two possible behaviors for the antiproton (curves 1 and 1*). Curve 4 is reported, too. Curve 1* in the figure corresponds to $\alpha = 1.24$, $\beta = 0.3$, $\gamma = 5 \times 10^5$, and represents the best approximation to the experimental data in the energy region beyond the maximum stopping power.

To give a quantitative estimation of the Barkas effect for the sample at 150 mbar we have drawn in Figs. 4(a), 4(c), 4(e), and 4(g) the experimental points $(z_{\text{exp}}, t_{\text{exp}})$ with the $t = f(z)$ functions built as follows. We have used the best fit curve 1 until its intersection with the proton curve (≈ 250 keV) and then the proton curve [Fig. 4(a)] or curve 4 [Fig. 4(c)]. The result has to be compared to the one obtained from curve 1 [Fig. 4(e)]. In Figs. 4(b), 4(d), and 4(f) we show the difference between the experimental and the fitted annihilation times of Figs. 4(a), 4(c), and 4(e) versus the respective experimental path lengths, with the interpolating straight line to guide the eye. In such a presentation it is directly evident that our data possess the required accuracy (some percent) to identify and evaluate the effect [9].

First of all, one may see that in Figs. 4(b) and 4(d) the points cross the zero in an opposite direction as compared to Figs. 4(a) and 4(c), respectively. Moreover, in Figs. 4(g) and 4(h) we report the corresponding behavior for curve 1*. It is possible to appreciate the difference with respect to curve 1 in Figs. 4(e) and 4(f).

In Fig. 2(b) we observe the maximum effect in the energy region around 600 keV. The difference in stopping power $S_{\bar{p}} - S_p$ turns to be $21\% \pm 3\%$ for this kinetic energy. This estimate results from the difference between the two values for curve 1 (2.0) and curve 1* (2.1) with respect to the proton value (1.7) ($\simeq 18\%$ and 24%,

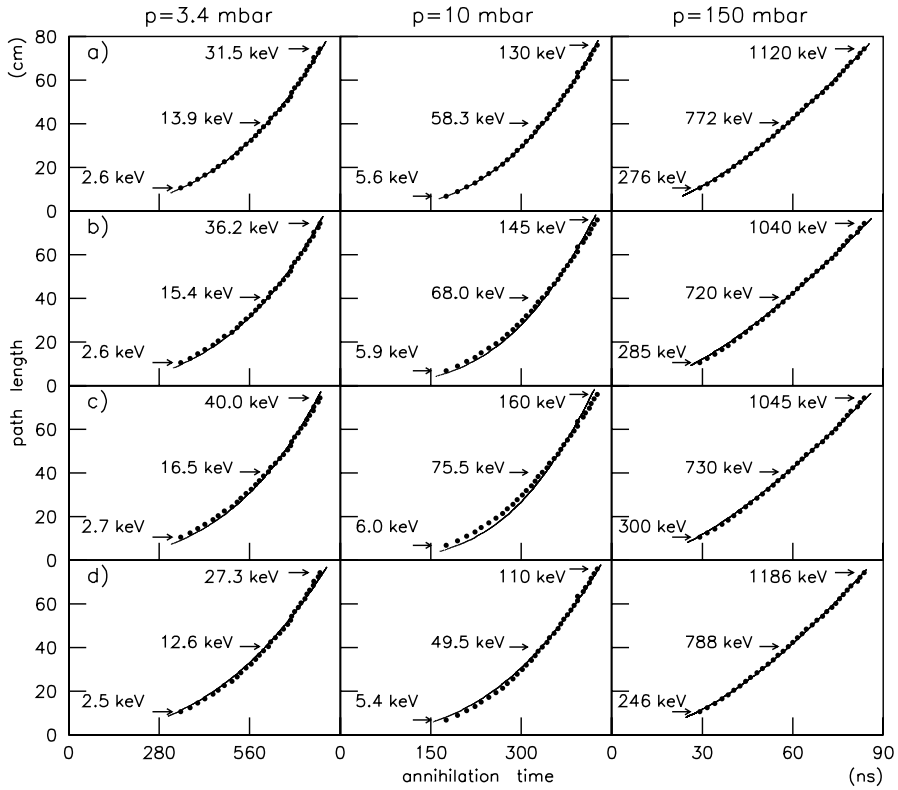

FIG. 3. $\bar{p}$ path length versus mean annihilation time with best fit curves at different H_2 pressures and $E_{\text{cap}} = 40$ eV. From top to bottom: (a) curve 1, (b) curve 2, (c) curve 3, (d) curve 4. The arrows indicate the E_i initial kinetic energy values for the $\bar{p}$ stopping in the gas near the entrance, in the middle, and near the exit wall of the target.

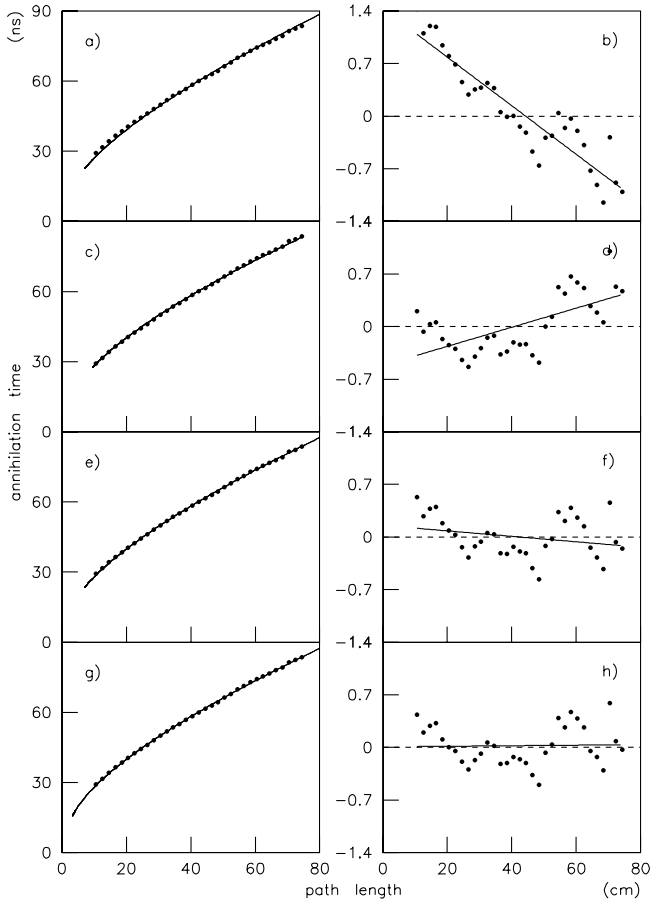

FIG. 4. Left column: mean $\bar{p}$ annihilation time versus path length at 150 mbar with the best fit curve 1 + proton (a), 1 + 4 (c), 1 (e), 1 + 1* (g); see text. Right column: annihilation time differences (ns) for experimental and best fit curves at different z in the target for the four curves in the left column.

respectively) and between curves 1 and 1* ($\simeq 15\%$ of the above difference). The values are in $S(E)$ units (see Fig. 2). This difference is nearly constant in the energy interval 400–700 keV, and tends to vanish beyond 3 MeV, where the $\bar{p}$ stopping power merges with the proton stopping power, as predicted by the first Born approximation. The Ermolaev analysis [7,8] yields higher values for the $\bar{p}$ ionization energy loss in atomic hydrogen, as compared to the proton, in the energy range 500 keV–3 MeV, reaching a difference of 10% at 1 MeV kinetic energy. We add the cross section for single ionization to the cross section for dissociative ionization of molecular hydrogen as measured by Hvelplund *et al.* [14]. This results in an antiproton cross section of 0.67 Å^2 and a proton cross section of 0.62 Å^2 at 600 keV corresponding to a difference of 8%. This result supports qualitatively the findings of the present work. As far as the Z dependence of the effect is concerned, the normal Barkas effect was observed in $\bar{p}$Si [15] and $\bar{p}$Au [16] collisions in the 200 keV–3 MeV interval. Measurements below 700 keV and below 100 keV on different medium-heavy solid targets are also reported in [17,18].

In conclusion, the behavior with energy of the Barkas effect and the properties of the nuclear stopping power (in particular the difference between the H_2 and the D_2 nuclear stopping power [3]), illustrate the extraordinary opportunity in using the antiproton as a projectile in media, the antiproton being the theorist's favorite low energy projectile. Such an antiparticle has made possible searches of important atomic processes more or less 90 years after the first paper of Niels Bohr "On the Theory of the Decrease of Velocity of Moving Electrified Particles on Passing through Matter" [19], where "the different conceptions in respect to the calculation of Sir J. J. Thomson" were presented.

*Corresponding author.
Email address: lodi@bs.infn.it

[1] A. Adamo *et al.*, Phys. Rev. A **47**, 4517 (1993).
[2] M. Agnello *et al.*, Phys. Rev. Lett. **74**, 371 (1995).
[3] A. Bertin *et al.*, Phys. Rev. A **54**, 5441 (1996).
[4] A. S. Wightman, Phys. Rev. **77**, 521 (1950).
[5] W. H. Barkas, J. N. Dyer, and H. H. Heckman, Phys. Rev. Lett. **11**, 26 (1963).
[6] T. B. Quinteros and J. F. Reading, Nucl. Instrum. Methods Phys. Res., Sect. B **53**, 363 (1991), and references therein.
[7] A. M. Ermolaev, Phys. Lett. A **149**, 151 (1990).
[8] A. M. Ermolaev, J. Phys. B **23**, L45 (1990).
[9] N. P. Frandsen *et al.*, *XVIII I.C.P.E.A.C., Abstract of Contributed Papers* (Aarhus University Press, Aarhus, 1993) Vol. II, p. 397.
[10] J. F. Reading (private communication): in atomic hydrogen with only one electron the effect is evaluated as very low or completely absent.
[11] J. S. Cohen, Phys. Rev. A **62**, 022512 (2000), and references therein.
[12] H. H. Andersen and J. F. Ziegler, *Hydrogen Stopping Powers and Ranges in All Elements* (Pergamon, New York, 1977).
[13] C. Varelas and J. P. Biersack, Nucl. Instrum. Methods **79**, 213 (1970).
[14] P. Hvelplund, H. Knudsen, U. Mikkelsen, E. Morenzoni, S. P. Møller, E. Uggerhøj, and T. Worm, J. Phys. B **27**, 925 (1994).
[15] R. Medenwaldt, S. P. Møller, E. Uggerhøj, T. Worm, P. Hvelplund, H. Knudsen, K. Elsener, and E. Morenzoni, Phys. Lett. A **155**, 155 (1991).
[16] S. P. Møller, Nucl. Instrum. Methods Phys. Res., Sect. B **48**, 1 (1990).
[17] S. P. Møller, E. Uggerhøj, H. Bluhme, H. Knudsen, U. Mikkelsen, K. Paludan, and E. Morenzoni, Phys. Rev. A **56**, 2930 (1997).
[18] S. P. Møller, A. Csete, T. Ichioka, H. Knudsen, U. I. Uggerhøj, and H. H. Andersen, Phys. Rev. Lett. **88**, 193201 (2002).
[19] N. Bohr, Philos. Mag. **25**, 10 (1913).